LAWRENCE
LIVERMORE
NATIONAL
LABORATORY

UCRL-PROC-217783

A Detailed Chemical Kinetic Model for TNT

William J. Pitz, Charles K. Westbrook

December 16, 2005

31st International Combustion Symposium
Heildelberg, Germany
August 6, 2006 through August 11, 2006

A Detailed Chemical Kinetic Model for TNT

William J. Pitz and Charles K. Westbrook

Lawrence Livermore National Laboratory, P.O. Box 808, Livermore, CA 94550

Manuscript submitted to 31st International Symposium on Combustion
Heidelberg, Germany
July 2006

Corresponding author: Charles K. Westbrook
Lawrence Livermore National Laboratory, L-090
P. O. Box 808
Livermore, CA 94551 USA
Fax: 925-423-8772
email: westbrook1@llnl.gov

Colloquium: Detonations, Explosions & Supersonic Combustion

Supplemental data included

Total Length of paper:
Method of determination: Method 1

Main text:	3684
References:	559
Figure 1:	160
Figure 2:	127
Figure 3:	249
Figure 4:	116
Figure 5:	115
Figure 6:	206
Table 1:	304
Table 2:	210
Total:	5734

A Detailed Chemical Kinetic Model for TNT

William J. Pitz and Charles K. Westbrook

Lawrence Livermore National Laboratory, P.O. Box 808, Livermore, CA 94550

Abstract

A detailed chemical kinetic mechanism for gas-phase combustion of 2,4,6-tri-nitrotoluene (TNT) has been developed to explore problems of explosive performance and of soot formation during the destruction of munitions. Thermodynamic properties of intermediate and radical species are estimated by group additivity. Reactions for the decomposition and oxidation of TNT and its intermediate products are assembled, based on information from the literature and from analogous reactions where the rate constants are available. The resulting detailed reaction mechanism for TNT is added to existing reaction mechanisms for RDX and for hydrocarbons which can be produced from TNT and RDX. Properties of the reaction mechanism are demonstrated by examining problems of soot formation during open burning of TNT and mixtures of TNT and RDX. Computed results show how addition of oxygen to TNT can reduce the amounts of soot formed in its combustion and why RDX and most mixtures of RDX and TNT do not produce soot during their combustion or incineration.

Introduction

Chemical kinetic modeling has become a valuable tool to assist in design and analysis of experiments and practical operations involving reactive materials. While early kinetic models were limited to small hydrocarbon and other related fuel molecules, steady growth in computing capabilities and in chemical theory has begun to make it possible to model fuels as complex as aromatic hydrocarbons [1] and large aliphatic molecules with 10 or more carbon atoms [2]. This growth in capabilities means that kinetic models for many new types of fuels are therefore possible, including a variety of fuels characterized as propellants, explosives and energetic materials. This study describes the development of such a detailed chemical kinetic reaction mechanism for the oxidation of 2,4,6-tri-nitrotoluene (TNT).

There are many potential uses of this type of combustion reaction mechanism for TNT. In particular, destruction of outdated munitions is often carried out by combustion, either via enclosed incineration, or by open burning or detonation. Soot production and emissions during open combustion have become serious environmental problems in some locations, and kinetic modeling of such soot production may offer some valuable insights. There is also a continuing need from users of explosives to improve their performance as well as ensure their safety against accidental initiation. Based on experience with smaller conventional hydrocarbon fuels, kinetic modeling is likely to provide valuable tools to assist in solving these problems.

Major obstacles exist for developing kinetic mechanisms for explosives. Most explosives include more types of atoms than are present in familiar hydrocarbons, including N atoms in the form of nitro and amino groups. Figure 1 shows some

important explosives molecules and illustrates the considerable presence of N atoms and the complexity of the molecular structures. TNT and TATB (tri-amino, tri-nitro benzene) are built on aromatic rings with multiple substituted branches with N atoms, and RDX and HMX are built upon rings with alternating C and N atoms, rather than aromatic rings, with nitro groups attached to each N atom in the ring. These are large, complex molecules, and the current frontier of kinetic combustion modeling is at this same level of chemical complexity. As a result, reaction mechanisms for these species are as large and complex as any currently being developed in conventional energy applications.

The extreme energy content of these explosives molecules means that they react so rapidly and violently that careful laboratory experiments are extremely difficult or dangerous, so the available experimental database is quite small for comparisons with computed results, and phenomenological observations are sometimes the only diagnostics available. Finally, all of the high explosives shown above are solids at room temperature and pressure, making their atmospheric combustion a multiphase technical problem. Such heterogeneous, multiphase problems are also at the frontier of combustion simulations [3].

Kinetic Model Development

Previous high explosive kinetic reaction mechanisms have been developed for only a few gas phase and condensed phase explosives. Tieszen et al. [4] developed kinetic models for hexyl nitrate and nitroethane and used them to predict ignition and detonation cell sizes for use in fuel/air explosives**.** Melius [5] developed the first detailed mechanism for any of the compounds in Fig. 1, adding reactions of RDX and its products

to a relatively simple hydrocarbon model and using it to model the RDX flame of Ermolin et al. [6]. Prasad, Yetter and Smooke [7] further developed the kinetic model for RDX, modeling both liquid and gas phase kinetics. They used their model to simulate the flame structure of a laser-supported RDX flame [8].

The present modeling study was motivated by two factors, both of which led to the selection of TNT as a model high explosive fuel. TNT is based on the aromatic ring hydrocarbon toluene, which has been the subject of our recent kinetic modeling attention [9], which thereby provides a core reaction mechanism on which to build a TNT model. In addition, some particularly important practical explosives consist of mixtures of RDX and TNT; for example, CompB is made of 40% TNT and 60% RDX, so the availability of a TNT reaction mechanism in addition to the existing RDX model would make it possible to simulate CompB kinetics as well as TNT and RDX individually.

Thermochemical parameters for new species were estimated using principles of group additivity, using the THERM code of Ritter and Bozzelli [10,11] to calculate heats and enthalpies of formation and temperature-dependent specific heats. Some groups were corrected to reflect heat of formation values in the literature. For example, the heat of formation for the CB/NO_2 group was corrected by 4.4 kcal/mole to give the heat of formation for nitrobenzene (16.38 kcal/mole) in the NIST database [12]. The NIST value agrees with the calculated BAC/MP4 value (14.18 kcal/mole) of Melius [13] after correcting a 2 kcal/mole BAC/MP4 systematic error for the benzene ring. However, for a considerable fraction of the 30 new species required, no previous thermochemical data were available. A representative sample of this data is summarized in Table 1.

In similar fashion, rates of elementary reactions were estimated when possible on the basis of known reactions for related species, drawing heavily on the work of Brill and James [14] and Tsang et al. [15,16]. For example, the principal initiation reaction for TNT at elevated temperatures involves breaking a C - N bond to produce NO_2 . The rate constant used in the present model, k_{TNT}, was based on the measured rate constants of the analogous reaction of 2-nitro-toluene (2-NT) and 4-nitro-toluene (4-NT) measured by Tsang et al. in a shock tube [15]. Since TNT has two groups ortho to the methyl and one group para to the methyl (see Fig. 1), the rate constant was assumed to be: $k_{TNT} = 2k_{2\text{-nt}} + k_{4\text{-nt}}$. This reaction was found to be the primary reaction consuming TNT in the simulations described below in this high temperature, gas phase study.

Two of the nitro groups in TNT are ortho to the methyl group, and He et al. [16] have discussed an initiation reaction for ortho-nitrotoluenes in which they suggest an H atom transfer from the methyl group to the nitro group, followed by elimination of a water molecule and resulting in the relatively unstable species anthranil. The anthranil will decompose rapidly to smaller species. This process has a low activation energy and could be the dominant initiation reaction for TNT and other o-nitrotoluenes at low and intermediate temperatures. It is also likely to be overtaken by the C - N bond-breaking reaction described above as temperature increases. We have not yet included this reaction step in our TNT mechanism, but it will be added when we begin to apply the mechanism to additional problems. Since the focus of the present application is the final product distribution following partial oxidation, this alternative initiation reaction is not expected to affect the conclusions of this illustration problem.

Additional reactions were added to the mechanism for isomerization of the -NO_2 group to -ONO and for breaking a C-CH_3 bond. These reactions were minor contributors to TNT consumption under the conditions of this study. A similar example of a rate constant estimate is the subsequent reaction of the methyl-di-nitrophenyl radical (DNTJ) produced by the major initiation step. Its reaction with NO_2 leaves an O atom on the phenyl radical site and an NO product, shown in Fig. 2. The analogous reaction of phenyl and NO_2 was studied by Preidel and Zellner [17], and their rate was used for the new reaction in the TNT mechanism.

Rates of H atom abstraction reactions in TNT were estimated as equal to H atom abstractions in toluene, again corrected for the relative numbers of available H atoms. Other reaction rates, particularly for radical decomposition reactions and for complex addition/decomposition reactions, were estimated based on the rates of reverse addition reactions and the relevant equilibrium constants. A total of 47 new elementary reactions were included to describe the reaction pathways involving TNT and its unique radicals and products. Examples of selected reactions with their modified Arrhenius rate coefficients are shown in Table 2.

This reaction mechanism is intended to describe combustion processes for TNT at atmospheric pressures, including open burning and other combustion applications, but it would require further development for applications at extremely high pressures, such as those expected in condensed phase detonations. The present mechanism would then be a subset of a more comprehensive model that would incorporate additional reaction steps, especially intramolecular processes that could be very important at very high densities.

The current reaction mechanism, including the portions describing TNT and RDX, includes 331 chemical species and 1679 elementary chemical reactions, and the overall reaction mechanism and thermochemistry data are available as supplemental data.

Model Applications

The specific application chosen to test the TNT reaction mechanism is the problem of soot production during open destruction of old munitions. In a typical case, explosives are placed on the ground in an open area and ignited, burning very rapidly and often accompanied by a large soot plume. An example of one experiment is shown in Figure 3, with the immediate reaction followed by a picture of the soot plume. While much of the plume consists of entrained dirt, a significant amount of soot is also present. In this and similar experiments, ignition is accomplished by detonation of a small charge which initiates the overall reaction of the TNT, and air and dirt are entrained during the subsequent combustion of the remaining explosives. Our goal is to simulate the production of soot during this combustion event and suggest modifications to the process to minimize soot production. This is a very complex combustion problem if treated in its entirety, since the explosives are usually present in multiple discrete units such as shell casings, so the fuel is extremely heterogeneous, initially in condensed phase, and in a complex geometry. In addition, the explosives are present initially in the solid phase and then vaporized during the incineration. However, since the present task is limited to understanding the nature of soot production during the combustion, a number of simplifying assumptions can be made. Based on previous experience with chemical kinetic simulations of soot production in diesel engine environments and methods of

reducing soot emissions, these simplifications can focus on the chemical factors involved and avoid the complications that are peripheral to the present problem.

Soot Production from Diesel Fuel and Explosives

At first glance, the combustion of explosives appears vastly different from most other classes of practical combustion, but on a closer inspection, there are interesting parallels with other systems that have been found to be valuable in guiding our analysis. Like other condensed phase fuels such as wood, coal, diesel fuel and many others, explosives are generally not mixed with oxidizer prior to the combustion event and depend on the addition of an oxidizer, usually air, to facilitate relatively complete combustion, and all of these fuels produce soot if sufficient oxidizer is not available. We have had success using an idealized kinetic modeling approach to describe soot formation in diesel combustion, as well as showing how soot production can be reduced or eliminated by varying the access of oxygen to the reacting fuel [18-21]. In this paper, we apply the same type of analysis to see how well the same processes and principles can be used to predict soot production during explosives combustion.

In our past work on diesel combustion, we assumed that, although the fuel is present initially in the condensed (i.e., liquid) phase, it vaporizes and entrains enough air to produce a very fuel-rich mixture that ignites at an initial temperature of about 900K. The fuel-rich mixture consumes all of the available oxygen and results in a hot (~1600-2000K) mixture of CO, H_2 and unsaturated hydrocarbon fragments such as acetylene, ethylene, and others that, due to the absence of more oxygen, cannot be oxidized further. These hot products then proceed to produce small aromatic hydrocarbons and then soot,

along reaction pathways that are becoming quite well established [22-25]. Note that in this analysis, the vaporization and air entrainment processes were not included in the modeling analysis, and all of the attention was devoted to the kinetics of the fuel-rich combustion and the identification of the products of that rich burn [26]. In spite of the great deal of problem simplification, this analysis has been able to show how variations in the fuel molecular structure [20], addition of other fuels containing additional oxygen atoms [19], entrainment of additional air prior to combustion [20,27], and other effects can have significant impacts on the amount of soot production, even eliminating soot production entirely.

In the present case of explosives combustion, most of the same analysis can be applied. For the present study, we begin with the combustion of TNT itself, without any air entrainment or presence of other chemical species prior to ignition. The products of this reaction are identified, using the kinetic model and the relation of these products to known pathways for soot production are described. Subsequently, the same combustion is simulated where increasing amounts of oxygen are added to the TNT, showing how increased availability of oxygen reduces soot production and eventually, when a large enough amount of oxygen is added, soot production is completely suppressed. In a following series of kinetic model calculations, the combustion of mixtures of TNT and RDX are considered, and we show that if sufficient RDX is present, soot production from TNT combustion is again suppressed. Just as in the diesel simulations, we carry out all of these calculations in the gas phase, in this case assuming that ignition from the first TNT to burn or from an outside source vaporizes much of the TNT. In cases with additional oxidizer (air) present, we assume that this oxidizer has been either entrained prior to its

combustion or was present initially as part of a multicomponent mixture of explosive and other species. Therefore these are homogeneous gas phase modeling calculations and are intended to illustrate the kinetic processes occurring rather than simulate all of the fluid mechanics and multiphase phenomena involved.

A considerable body of kinetic research has established that soot is produced primarily by the growth of large polycyclic aromatic hydrocarbon species that grow by addition of small, usually unsaturated hydrocarbon fragments and molecules. Acetylene and hydrogen, together with vinyl, propargyl and methyl-allyl radicals are particularly effective species for soot inception and growth [22,23,25]. Sooting fuels have significant amounts of these soot precursors in the post-ignition pool of chemical species, while non-sooting fuels have very small concentrations of these soot precursors.

Results for Soot Production in TNT Combustion

The combustion of a homogeneous gas phase sample of TNT was simulated computationally using the kinetic mechanism already described. Following an ignition delay of 0.4 s, the sample ignited and the TNT was oxidized until all of the O atoms originally in the TNT were depleted (mostly forming CO), at which time the reaction was effectively quenched. The major features of the combustion of the TNT include initiation by breaking the C – NO_2 bond to form di-nitro-methyl-phenyl radical. The radical reacts with NO_2 to form di-nitro-methyl-phenoxy radical which decomposes to di-nitro-methyl-cyclopentadienyl radical and CO. The later radical undergoes another reaction with NO_2 to form di-nitro-methyl-cyclopentadienoxy radical which decomposes in multiple steps to form a methyl radical, an NO_2 and 2-nitro-2,4-cyclopentadien-4-yl-1-one radical.

This radical undergoes ring opening and further decomposition to form CO, NO_2 and two C_2H radicals. The net result from the reaction of one TNT molecule is $NO+NO_2+CH_3+2CO+2C_2H$. The C_2H radicals abstract an H atom from TNT for form acetylene which is a main contributor to soot growth reactions.

The mole fractions of all of the species identified with soot production, including acetylene, ethylene, benzene, toluene, and propene were summed at each time step in the simulation, with the results shown in Figure 4. The soot precursor level of about 1% at some time following the combustion is comparable with soot precursor levels calculated for diesel combustion environments. Virtually all of the soot precursors in the TNT model consist solely of acetylene, and the only significant other products are H_2 and CO, although small amounts of radical species including H, CH, CH_2, HCO and OH are also present. Evidently the oxidation of the TNT towards CO_2 and H_2O was simply interrupted by the consumption of all of the O atoms present initially in the TNT molecules, and the reacting mixture was effectively frozen at that point in the reaction.

While we did not model the subsequent production of soot from this mixture for the present work, many studies have confirmed [22,23,28] that soot will be produced quite easily from this type of mixture, with acetylene as the major soot growth species.

In order to understand the role of oxygen in the reactant mixture, we repeated this calculation with gradually larger fractions of O_2 in the reactant mixture. This addresses in a general way what might be expected if more air were entrained with the reacting fuel early in the combustion period. The levels of soot precursor species were steadily decreased as the O_2 level increased, as shown in Figure 5. Again, the only major

unsaturated hydrocarbon in the combustion products available to produce soot is acetylene. The predicted soot precursor level in these products reaches very low levels by the time the O_2 fraction in the reactants reaches about 30%, which is extremely consistent with results obtained in engine experiments and kinetic simulations of diesel combustion [18,29]. The additional O_2 effectively converts acetylene to CO and H_2, removing acetylene from the pool of chemical species available to produce soot.

In the diesel engine literature, the critical parameter is O/C in the fuel, the ratio of oxygen to carbon or, equivalently, the fraction of O in the fuel. Examination of the detailed kinetic results indicates that the key to eliminating soot production is to convert all of the available carbon in the fuel to CO, which requires that the ratio O/C be unity. Since there are 7 carbon atoms and 6 O atoms in TNT, O/C reaches unity for a mixture with the O_2 level approximately 33% of the (TNT + O_2) total concentration, and this is exactly the level shown in Fig. 5 for the disappearance of soot precursors. Another essential element to this analysis is the fact that, as shown in the kinetic results, all of the larger fuel molecules, in particular the TNT molecules, are completely broken down to small fragments during the rich ignition. It is the fraction of these small fragments that are converted into CO that is the essential process that determine the ability of the product mixture to produce soot.

When the same model calculations are repeated with RDX as the explosive fuel, the computed soot precursor concentrations are effectively zero, even without any O_2 addition to the RDX. This was found to be in good agreement with actual experimental observations that RDX is found to produce little or no soot when burned or detonated in

the open atmosphere [30]. An examination of the structure of RDX in Fig. 1 shows that there are no C - C bonds in RDX, so the production of species such as acetylene, ethylene and any others with C - C single or double bonds would be expected to be very small. Furthermore, the O/C ratio in RDX is equal to 2, so the criterion of $O/C \geq 1$ to facilitate conversion of fuel carbon to CO is easily accomplished.

Finally, it is quite common to produce explosives that mix more than one type of explosive molecule with another. CompB is a mixture of 40% TNT and 60% RDX. Simply by calculating the ratio of O/C as equal to about 1.25 for CompB suggests strongly that CompB would not produce significant amounts of soot. A detailed kinetics calculation, using both the RDX and TNT mechanisms, for various mixtures of these two components, confirms the simple prediction. As an example, Figure 6 shows the computed levels of soot precursors for mixtures of 90% TNT/10% RDX and at 80% TNT/20% RDX, showing that the soot precursors disappear in this interval. Actual calculation of the O/C ratio for these mixtures shows that O/C = 1 for a mixture of 87.5% TNT and 12.5% RDX, in good agreement with the detailed kinetic results.
A final observation on the amount of oxygen required to eliminate soot production by TNT is that the 30% O_2 indicated in Figure 5 is a molar percentage, which can be converted to a 1:1 volumetric ratio of solid TNT to gaseous oxygen if the oxygen is provided at 80 - 100 atm pressure, which is commonly available in pressurized laboratory gas containers. An array such as those in Fig. 3, with pressurized oxygen containers alternated with TNT munitions of similar overall size, might provide enough mixing between TNT and oxygen to significantly suppress soot production. This concept is awaiting experimental testing, although the required amounts of oxygen might be more

conveniently or more economically provided in other ways than in the form of pressurized containers.

Conclusions

A detailed chemical kinetic reaction mechanism has been developed for TNT, based on existing models for toluene, nitrobenzene, and other related species. The mechanism was used to study soot production during open combustion of TNT munitions, and the model predicted soot precursor levels consistent with experimental observations. Comparable calculations for a different high explosive, RDX, showed that unlike TNT, RDX produced no soot or soot precursors, again in excellent agreement with experimental observations. This combination of computed results gives good credibility to the new TNT reaction mechanism, but many additional model tests are necessary to validate and improve the reaction mechanism.

Acknowledgments

The authors thank Dr. C. F. Melius for helpful discussions on the chemical kinetic mechanism. The work was supported by the Joint DoD/DOE Munitions Technology Program and performed under the auspices of the U.S. Department of Energy by the University of California, Lawrence Livermore National Laboratory under Contract No.W-7405-Eng-48. The authors thank Jim Wheeler, Director of the U. S. Army's Defense Ammunition Center, and Bruce Watkins and Peter Hsu, LLNL program managers, for their support of this work.

References

1. R. Bounaceur, I. D. Costa, R. Fournet, F. Billaud and F. Battin-Leclerc, *Int. J. Chem. Kinet.* 37 (1) (2005) 25-49.
2. P. Dagaut, *Physical Chemistry Chemical Physics* 4 (11) (2002) 2079-2094.
3. C.K. Westbrook, Y. Mizobuchi, T. Poinsot, P.A. Smith, and J. Warnatz, *Proc. Combust. Inst.* 30 (2004) 125-157.
4. S.R. Tieszen, D.W. Stamps, C.K. Westbrook, and W.J. Pitz, *Combust. Flame* 84 (1990) 376-390.
5. C.F. Melius, in: S.N. Bulusu, (ed.), *Chemistry and Physics of Energetic Materials*, Kluwer Academic Publishers, The Netherlands, 1990, pp. 51-78.
6. N. E. Ermolin, O. P. Korobeinichev, L. V. Kuibida, and V. M. Fomin, *Fiz. Goreniya Vzryva* 22 (1986) 54.
7. K. Prasad, R.A. Yetter, and M.D. Smooke, *Combust. Sci. Technol.* 124 (1997) 35-82.
8. D. Hanson-Parr, and T. Parr, *Proc. Combust. Inst.* 25 (1994) 1635-1643.
9. W. J. Pitz, R. Seiser, J. W. Bozzelli, K. Seshadri, C.-J. Chen, I. D. Costa, R. Fournet, F. Billaud, F. Battin-Leclerc and C. K. Westbrook, *Chemical Kinetic Study of Toluene Oxidation under Premixed and Nonpremixed Conditions,* Lawrence Livermore National Laboratory, UCRL-CONF-201575, (2003).
10. E.R. Ritter, and J.W. Bozzelli, *Int. J. Chem. Kinetics* 23 (1991) 767-778.
11. T.H. Lay, J.W. Bozzelli, A.M. Dean, and E.R. Ritter, *J. Phys. Chem.* 99 (1995) 14514-14527.

12. NIST Chemistry WebBook, NIST Standard Reference Database Number 69, Eds. P.J. Linstrom and W.G. Mallard, March 2003, National Institute of Standards and Technology, Gaithersburg MD, 20899 (http://webbook.nist.gov). Reference cited in NIST database is Pedley, J.B., Naylor, R.D., Kirby, S.P., Thermochemical Data of Organic Compounds, Chapman and Hall, New York, 1986.

13. C.F. Melius, in: S. N. Bulusu, (ed.) *Chemistry and Physics of Energetic Materials*, Kluwer Academic Publishers, The Netherlands, 1990, pp.21-49.

14. T.B. Brill, and K.J. James, *Chem. Rev.* 93 (1993) 2667-2692.

15. W. Tsang, D. Robaugh, and W.G. Mallard, *J. Phys. Chem.* 90 (1986) 5968-5973.

16. Y.Z. He, J.P. Cui, W.G. Mallard, and W. Tsang, *J. Am. Chem. Soc.* 110 (1988) 3754-3759.

17. M. Preidel, and R. Zellner, *Ber. Bunsenges. Phys. Chem.* 93 (1989) 1417 (1989).

18. P.F. Flynn, R.P. Durrett, G.L. Hunter, A.O. zur Loye, O.C. Akinyemi, J.E. Dec, and C.K. Westbrook, *Soc. Auto. Engin. Trans.* 108 (1999) 587-600.

19. H.J. Curran, E.M. Fisher, P.A. Glaude, N.M. Marinov, W.J. Pitz, C.K. Westbrook, D.W. Layton, P.F. Flynn, R.P. Durrett, A.O. zur Loye, O.C. Akinyemi, and F.L. Dryer, *Soc. Auto. Engin. Trans.* 110 (2001) 514-521.

20. C.J. Mueller, W.J. Pitz, L.M. Pickett, G.C. Martin, D.L. Siebers, and C.K. Westbrook, *Soc. Auto. Engin. SAE* 2003-01-1791 (2003).

21. B.A. Buchholz, C.J. Mueller, A. Upatnieks, G.C. Martin, W.J. Pitz, and C.K. Westbrook, *Soc. Auto. Engin. SAE* 2004-01-1849 (2004).

22. M. Frenklach and H. Wang, *Combust. Flame* 110 (1997) 173-221.

23. J.A. Miller, M.J. Pilling and J. Troe, *Proc. Combust. Inst.* 30 (2005) 43-88.

24. H. Richter and J.B. Howard, *Prog. Energy Combust. Sci.* 26 (2000) 565-608.

25. J.A. Miller, and C.F. Melius, *Combust. Flame* 91 (1992) 21-39.

26. J.E. Dec, *Soc. Auto. Engin.* SAE 970873 (1997).

27. D. Siebers, and B. Higgins, *Soc.Auto. Engin. SAE* 2002-01-0530 (2001).

28. S.J. Harris, A.M. Weiner, R.J. Blint and J.E.M. Goldsmith, *Proc. Combust. Inst.* 21 (1986) 1033-1045.

29. N. Miyamoto, H. Ogawa, N.M. Nurun, K. Obata, and T. Arima, *Soc. Auto. Engin. SAE* 980506 (1998).

30. C.M. Tarver, personal communication (2004).

Supplemental data

List of files:

tnt_v1j_tol_v6k_rdx_1a_c4_2c.mech	text file of TNT mechanism in CHEMKIN format
tnt_v1g_rdx_1b_ic8_2e_tolv6e.therm	text file of TNT thermodynamic properties in CHEMKIN format

SPECIES	Hf	S	Cp 300
TNT	1.55	112.64	52.12
TNBENZYL	38.45	110.08	52.87
TNTJ	62.45	114.12	51.71
DNT	4.97	101.15	43.10
DNTJ	65.87	102.63	42.69
NT	8.39	89.67	34.08
NT-2	8.39	89.67	34.08
DNTOH	-37.13	108.52	48.06
DNT-OJ	-2.73	109.82	46.48
TNPH	9.54	100.07	46.50
TNPHJ	70.44	103.73	46.09
MEDNCP	9.68	69.56	30.83
MEDNCPDJ	35.58	70.84	31.12
TNPHC*O	-19.16	117.70	54.30
TNPHCJ*O	15.74	116.31	54.11
TNPHOH	-32.56	109.62	51.46
TNPHOJ	1.84	110.92	49.88
C#CC*CNO2	35.45	77.15	22.60
C#CC*CJN	94.55	78.54	22.41

Table I. Thermochemical data for some species included in TNT kinetic reaction mechanism. Hf=enthalpy of formation at 298K in kcal/mole, S=enthalpy at 298K in cal/mole-K, Cp = specific heat at constant pressure in cal/mole-K.
(TNT = 2,4,6-tri-nitrotoluene, TNBENZYL = 2,4-6-tri-nitrobenzyl radical, TNTJ = 1-methyl-2,4,6-trinitrophenyl radical, DNT = 2,4-di-nitrotoluene, DNTJ = 1-methyl-4,6-di-nitrophenyl radical, NT = nitrotoluene, TN-2 = 2-nitrotoluene, DNTOH = 2-methyl-3,5-nitro-phenol, DNT-OJ = 2-methyl-3,5-nitro-phenoxy, TNPH = 1,3,5-tri-nitro-benzene, TNPHJ = 1,3,5-tri-nitro-phenyl, MEDNCP = 1,3-nitro-5-methyl-1,3-cyclopentadiene, MEDNCPDJ = 1,3-nitro-5-methyl-1,3-cyclopentadienyl radical, TNPHCJ*O = 2,4,6-tri-nitro-phenyl-formyl radical, TNPHOH = 2,4,6-tri-nitrophenol, TNPHOJ = 2,4,6-tri-nitrophenoxy, C#CC*CNO2 = 1-nitro-2-ethynyl-ethene, C#CC*CJN = 1-nitro-2-ethynyl-vin-1-yl)

	A	n	Ea (cal)
tnt+o2=tnbenzyl+ho2	9.30E+08	1.3	40939
tnt=dntj+no2	8.54E+14	0.0	61470
tnt=tnphj+ch3	7.94E+16	0.0	104000
tnt=dnt-ono	1.00E+13	0.0	55980
dnt-oj+no=dnt-ono	5.44E+13	-0.7	0
tnt=tnbenzyl+h	3.10E+15	0.0	89210
tnt+h=dnt+no2	7.57E+18	-1.7	6410
dnt+h=nt+no2	5.05E+18	-1.7	6410
nt+h=c6h5ch3+no2	2.52E+18	-1.7	6410
tnt+h=tnph+ch3	7.57E+18	-1.7	6410
tnt+oh=tnbenzyl+h2o	5.19E+09	1.0	874
tnt+h=tnbenzyl+h2	4.00E+02	3.4	3120
tnt+ch3=tnbenzyl+ch4	2.21E+00	3.5	5675
tnt+o=tnbenzyl+oh	6.00E+10	0.7	7632
tnt+ho2=tnbenzyl+h2o2	1.02E+04	2.5	12340
tnt+no2=tnbenzyl+hono	1.20E+13	0.0	30000
tnt+h=dntj+hono	3.18E+15	0.0	15700

Table II. Modified Arrhenius coefficients for selected reactions in TNT mechanism. Units are cal-mole-sec.

(dnt-ono = 2-methyl-3,5-nitro-phenylnitrite. The other species are identified in Table I).

Figure captions

Figure 1. Four common high explosives molecules in common use.

Figure 2. Reaction of dinitrobenzyl radical with NO_2 (upper), and analogous reaction (lower) of phenyl radical [13].

Figure 3. Open detonation of TNT. Upper figure shows ignition and early burn, lower figure shows entrained cloud of dirt and soot.

Figure 4. Time dependence of soot precursors during rich burn of TNT, with no added oxygen.

Figure 5. Computed variation in residual soot precursors with added oxygen in TNT ignition

Figure 6. Soot precursors in TNT/RDX mixtures. Top figure is for 80% TNT/20% RDX, bottom figure is for 90% TNT/10% RDX

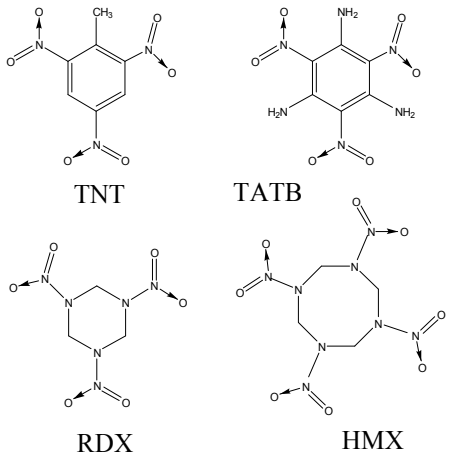

Figure 1

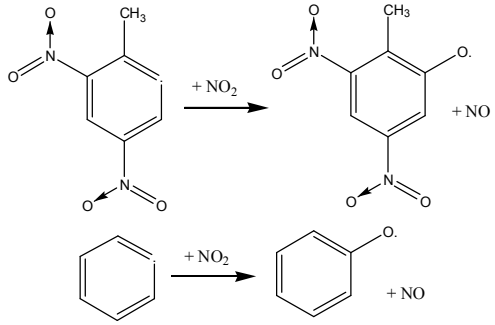

Figure 2

Figure 3

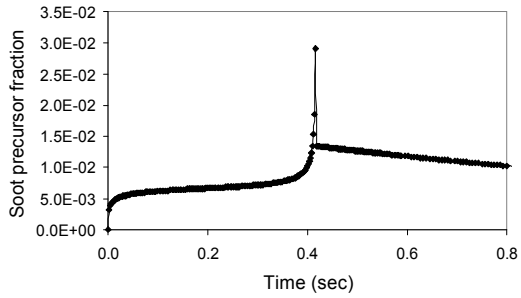

Figure 4.

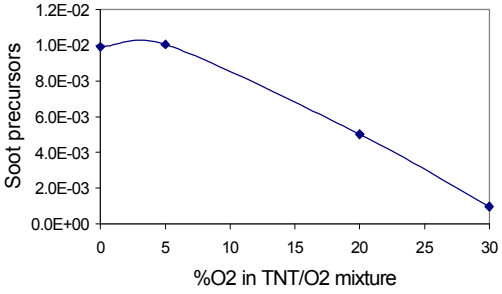

Figure 5

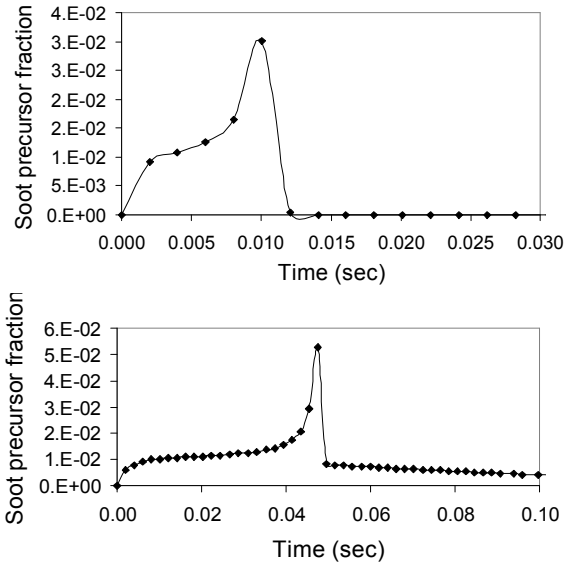
Soot precursor fraction
4.E-02
3.E-02
3.E-02
2.E-02
2.E-02
1.E-02
5.E-03
0.E+00
0.000
0.005
0.010
0.015
0.020
0.025
0.030
Time (sec)
Soot precursor fraction
6.E-02
5.E-02
4.E-02
3.E-02
2.E-02
1.E-02
0.E+00
0.00
0.02
0.04
0.06
0.08
0.10
Time (sec)

Figure 6